Inorg. Chem. **2004**, *43*, 7308–7314

DOTP–Manganese and –Nickel Complexes: from a Tetrahedral Network with 12-Membered Rings to an Ionic Phosphonate

Deyuan Kong, Dmitri G. Medvedev, and Abraham Clearfield*

Department of Chemistry, Texas A&M University, College Station, Texas 77842-30012

Received June 7, 2004

DOTP (1,4,7,10-tetrakis(methylenephosphonic acid)-1,4,7,10-tetraazacyclododecane) was reacted hydrothermally with $MnCl_2 \cdot 2H_2O$ and $Ni(NO_3)_2 \cdot 6H_2O$ resulting in two structurally different compounds. $Mn[C_3NH_7(PO_3H_{0.5})]_4$ crystallizes in the tetragonal space group *P*4/*ncc*, with $a = 12.349(2)$ Å, $b = 12.349(2)$ Å, $c = 14.066(4)$ Å, $V = 2144.9(8)$ Å^3, and $Z = 4$. Manganese atoms are tetrahedrally bonded by four phosphonate oxygen atoms from four equivalent ligands. All 12-membered macrocycles are connected in a "zigzag" manner by sharing manganese atoms and forming 22-membered cavities between each pair of two adjacent macrocycles. $Ni[C_3NH_6(PO_3H)]_4[Ni(H_2O)_6]$ crystallizes as an ion pair complex. Ni(1) is octahedrally coordinated to two pendent phosphonate oxygen atoms and four nitrogen atoms from the macrocyclic backbone. Ni(2) is surrounded by six coordinatedly bonded water molecules to form a hexaqua cation. The manganese complex shows ion exchange capability for Cs^+.

Introduction

The chemistry of the metal phosphonates has been a research field of rapid expansion in recent years, mainly due to their potential application in the areas of catalysis, ion exchange, proton conductivity, intercalation chemistry, photochemistry, and materials chemistry.[1] Most of the metal phosphonates have a layered structure in which the metal centers are bridged by the phosphonate group, although a variety of 1D chains and porous 3D networks have also been reported. The main obstacle in metal phosphonate chemistry is the fact that many metal phosphonates of tetravalent metals normally form poorly crystalline compounds, making their structural studies a rather difficult task. Phosphonic acids with additional functional groups such as aza-crown ethers, amines, and carboxylic groups have been found to be better ligands since they can provide more coordination sites that may not only increase the solubility of the metal phosphonates in water and improve the crystallinity of their metal complexes, but also form many complexes with novel structures.[2−4] The reaction of metal(II) salts with an aza-crown ether resulted in a number of "macrocyclic leaflets" with a 1D chain structures as well as other structural moieties.[2] Several types of structures have been reported for metal complexes with H_4PMIDA under different pH conditions.[4] A number of metal phosphonocarboxylates have been reported; their structures normally feature either a 2D layer or a 3D network with an open framework.[5]

DOTP, 1,4,7,10-tetrakis(methylenephosphonic acid)-1,4,7,-10-tetraazacyclododecane, has proved to be a particularly favorable NMR shift reagent for the $^{23}Na^+$ NMR spectroscopic study of isolated cells, perfused tissues, and intact animals.[6] (See Scheme 1 for the ligand structure information.) It is also useful as an extracellular in vivo marker of tissues.[7] The relaxation properties of the Gd^{3+} complex, a potential MRI contrast agent, have also been reported.[8] The structures of the Ln^{3+} complexes of this ligand in solution have been thoroughly investigated using multinuclear NMR spectro-

* To whom correspondence should be addressed. E-mail: clearfield@mail.chem.tamu.edu.

(1) Clearfield, A. Metal Phosphonate Chemistry. In *Progress in Inorganic Chemistry*; Karlin, K. D.; Ed.; John Wiley & Sons: New York, 1998; Vol. 47, pp 371−510 and references therein.

(2) (a) Sharma, C. V. K.; Clearfield, A. *J. Am. Chem. Soc*. **2000**, *122*, 1558. (b) Clearfield, A.; Sharma, C. V. K.; Zhang, B. *Chem. Mater*. **2001**, *13*, 3099. (c) Mao, J. G.; Wang, Z.; Clearfield, A. *Inorg. Chem*. **2002**, *41*, 3713. (d) Clearfield, A. *Curr. Opin. Solid State Mater. Sci*. **2002**, *6*, 495.

(3) (a) Sharma, C. V. K.; Clearfield, A.; Cabeza, A.; Aranda, M. A. G.; Bruque, S. *J. Am. Chem. Soc*. **2001**, *123*, 2885. (b) Mao, J. G.; Wang, Z.; Clearfield, A. *Inorg. Chem*. **2002**, *41*, 2334. (c) Mao, J. G.; Wang, Z.; Clearfield, A. *New. J. Chem*. **2002**, *26*, 1010.

(4) (a) Poojary, D. M.; Zhang, B.; Clearfield, A. *Angew. Chem., Int. Ed. Engl*. **1994**, *33*, 2324. (b) Zhang, B.; Poojary, D. M.; Clearfield, A. *Inorg. Chem*. **1998**, *37*, 249. (c) Mao, J. G.; Clearfield, A. *Inorg. Chem*. **2002**, *41*, 2319. (d) Gutschke, S. O. H.; Price, D. J.; Powell, A. K.; Wood, P. T. *Angew. Chem., Int. Ed*. **1999**, *38*, 1088.

(5) (a) Stock, N.; Stucky, G. D.; Cheetham, A. K. *Chem. Commun*. **2000**, 2277. (b) Zhu, J.; Bu, X.; Feng, P.; Stucky, G. D. *J. Am. Chem. Soc*. **2000**, *122*, 11563 and references therein. (c) Zhang, B.; Clearfield, A. *J. Am. Chem. Soc*. **1997**, *119*, 2751.

10.1021/ic040076m CCC: $27.50
Published on Web 10/20/2004

Scheme 1. Synthetic Route for Compounds **1** and **2**

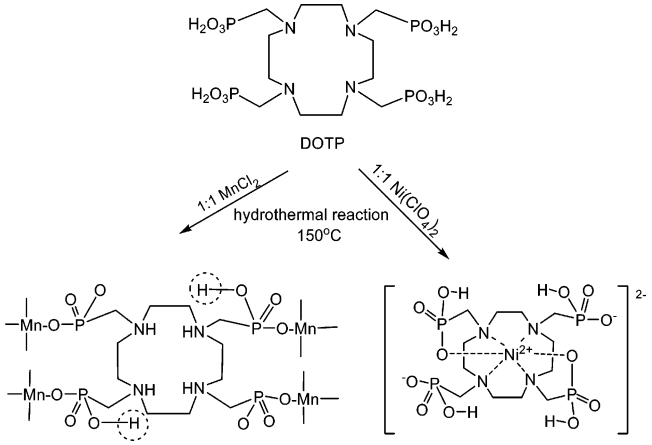

scopic techniques[9] and utilizing the structural information derived from the paramagnetic effects of these ions.[10] However, only a preliminary X-ray crystal structure of the $[(NH_4)_5Tm(DOTP)]$ complex has been reported.[11] Also, two recent single crystal structures of $[\{Na_{13}(OH)_3(H_2O)_{29}\}\{Gd(DOTP)\}][Gd(DOTP)]\cdot 7H_2O\cdot 2CH_3CH_2OH$[12] and $[Bi(H_4DOTP)(Na(H_2O)_4)]$ together with one powder structure of $[Bi(H_4DOTP)(H_5O_2)]$ were reported.[13] Transition metal phosphonates with this ligand are relatively rare. Most literature focuses on synthesis, thermodynamic stability, dissociation kinetics, metal selectivity, and coordination behavior.[14] The crystal structures of metal complexes have recently become of general interest in this area. To develop new inorganic−organic hybrid ion exchangers with immobilized crown ethers having novel properties, DOTP was hydrothermally treated with Mn^{2+} and Ni^{2+} ions. Two different types of structures were obtained: the Mn compound formed a 2D infinite sheet and the Ni crystallized as ion pair single molecules. Preliminary experiments showed that the Mn compound has the ability to ion exchange Cs^+.

Experimental Methods

The chemicals were purchased from commercial sources and used as received.

The IR spectra were recorded in KBr pellets on a Nicolet Nexus 470 FTIR spectrometer with spectral resolution of 2.00 cm^{-1}. Thermogravimetric studies were carried out with a TA instruments TGA Q-500 unit at a heating rate 10 °C/min under argon. SEM images were acquired at the Texas A&M University Microscopy and Imaging Center. The elemental analysis data were obtained from Robertson Microlit Laboratories, Madison, NJ. The DOTP ligand was synthesized and purified using procedures reported previously.[15] Magnetic susceptibility and magnetization measurements were carried out on a Quantum Design SQUID magnetometer MPMS-XL. Direct current magnetic measurements were performed with an applied field of 1000 G in the 2−300 K temperature range. Data were corrected for diamagnetic contributions calculated from the Pascal constants.

Synthesis of 1 and 2. Complex **1** was synthesized by a hydrothermal reaction. A total of 0.2 mmol of 1,4,7,10-tetrakis-(methylenephosphonic acid)-1,4,7,10-tetraazacyclododecane and 0.2 mmol of manganese chloride bishydrate (Aldrich) with 10.0 mL of deionized water was sealed into a Teflon pressure vessel, and heated at 150 °C for 24 h. Colorless needlelike crystals were recovered for **1** in ca. 77.6% (0.093 g) yield. Elemental analysis for **1**, $C_{12}H_{32}N_4O_{12}P_4Mn$: C, 23.81%; H, 4.64%; N, 9.07%. Calcd: C, 23.89%; H, 5.35%; N, 9.29%.

A similar synthesis was carried out for **2**, except that the ligand solution was neutralized with Et_3N and the pH adjusted to 6 before adding the nickel salt. The final product was obtained as green crystals ca. 48.7% (0.075 g) yield. $C_{12}H_{40}N_4O_{18}P_4Ni_2$: C, 19.51%; H, 4.99%; N, 7.03%. Calcd: C, 18.72%; H, 5.24%; N, 7.28%.

Crystallography. X-ray Structural Analyses. Data ($3.3° < \theta < 23.26°$, $2.18° < \theta < 28.31°$) were collected at 110 K on a Bruker Smart CCD-1000 platform diffractometer equipped with monochromated (Mo Kα, $\lambda = 0.71073$ Å) and OXFORD cool stream low-temperature control unit. Data collection and reduction were performed with a Bruker CCD Smart 5.4 and SAINT +6.0 from Bruker AXS.[16] Crystallographic computation was carried out using the SHELXTL 5.10 package.[17] The cell constants were indexed from reflections obtained from 60 frames with an exposure of 10 s/frame. A hemisphere of data (1271 frames at 5 cm detector distances) was collected by the narrow-frame method with frame widths of 0.03° in ω and exposure time of 40 s/frame. The first 50 frames were recorded at the end of data collection to assess the stability of the crystals, and the decay in intensity was found to be

(6) (a) Sherry, A. D.; Malloy, C. R.; Geraldes, F. G. C. C.; Cacheris, C. F. G. *J. Magn. Reson*. **1988**, *76*, 528. (b) Buster, D. C.; Castro, M. M. C. A.; Geraldes, F. G. C. C.; Malloy, C. R.; Sherry, A. D. *Magn. Reson. Med*. **1990**, *15*, 25. (c) Malloy, C. R.; Buster, D. C.; Castro, M. M. C. A.; Geraldes, F. G. C. C.; Geraldes, F. G. C. C.; Sherry, A. D. *Magn. Reson. Med*. **1990**, *15*, 33. (d) Butwell, N. B.; Ramasamy, R.; Sherry, A. D. *Invest. Radiol*. **1991**, *26*, 1079. (e) Butwell, N. B.; Ramasamy, R.; Lazar, I.; Malloy, C. R.; Sherry, A. D. *Am. J. Physiol.* **1993**, *264*, H1884. (f) Pike, M. M.; Luo, C. S.; Clark, M. D.; Kirk, K. A.; Kitakaze, M.; Madden, M. C.; Cragoe, E. J., Jr.; Pohost, G. M. *Am. J. Physiol.* **1993**, *265*, H2017. (g) Bansal, N.; Germann, M. J.; Lazar, I.; Sherry, A. D. *J. Magn. Reson. Imaging* **1992**, *2*, 385. (h) Bansal, N.; Germann, M. J.; Seshan, V.; Shires, G. T., III; Malloy, C. R.; Sherry, A. D. *Biochemistry* **1993**, *32*, 5638. (i) Xia, Z. F.; Horton, J. W.; Zhao, P. Y.; Bansal, B.; Babcock, E. E.; Sherry, A. D.; Malloy, C. R. *J. Appl. Physiol.* **1994**, *76*, 1507. (l) Seshan, V.; Germann, M. J.; Preising, P.; Malloy, C. R.; Sherry, A. D.; Bansal, B. *Magn. Reson. Med*. **1995**, *34*, 25.

(7) (a) Makos, J. D.; Malloy, C. R.; Sherry, A. D. *J. Appl. Physiol.* **1998**, *85*, 1800. (b) Geraldes, C. F. G. C.; Brown, R. D., III; Cacheris, W. P.; Koenig, S.; Sherry, A. D. *Magn. Reson. Med.* **1989**, *9*, 94.

(8) Aime, S.; Botta, M.; Terreno, E.; Anelli, P. L.; Uggeri, F. *Magn. Reson. Med*. **1993**, *30*, 583.

(9) (a) Aime, S.; Botta, M.; Terreno, P. D.; Williams, J. A. G. *J. Chem. Soc., Dalton Trans.* **1996**, 17. (b) Geraldes, C. F. G. C.; Sherry, A. D.; Kiefer, G. E. *J. Magn. Reson*. **1992**, *97*, 290. (c) Ren, J.; Sherry, A. D. *J. Magn. Reson*. **1996**, *B111*, 178. (d) Aime, S.; Botta, M.; Garino, E.; Crich, S. G.; Giovenzana, G. B.; Pagliarin, R.; Palmisano, G.; Sisti, M. *Chem. Eur. J.* **2000**, *6*, 2609. (e) Sherry, A. D.; Geraldes, C. F. G. C.; Cacheris, W. P. *Inorg. Chim. Acta* **1987**, *139*, 137.

(10) (a) Peters, J. A.; Huskens, J.; Raber, D. *Prog. Nucl. Magn. Reson. Spectrosc*. **1996**, *28*, 283. (b) Peters, J. A.; Zitha-Bovens, E.; Corsi, D. M.; Geraldes, F. G. C. C. In *The Chemistry of Contrast Agents in Medical Magnetic Resonance Imaging*; Merbach, A. E., Tóth, É., Eds.; John Wiley & Sons: Chichester, 2001; Chapter 8.

(11) Paulus, E. F.; Juretschke, P.; Lang, J. 3. Jahrestag Der Deutschen Gesellschaft für Kristallographie, Darmstadt, 1995.

(12) Avecill, F.; Peters, J. A.; Geraldes, F. G. C. C. *Eur. J. Inorg. Chem*. **2003**, 4179.

(13) Hassfjell, S.; Kongshaug, K. O.; Rømming, C. *J. Chem. Soc., Dalton Trans.* **2003**, 1433.

(14) Lukes, I.; Kotek, J.; Vojtisek, P.; Hermann, P. *Coord. Chem. Rev*. **2001**, *216−217*, 287.

(15) Lazar, I.; Hrncir, D.; Kim, W. D.; Kiefer, G. E.; Sherry, A. D. *Inorg. Chem*. **1992**, *31*, 4422.

(16) *SMART version 5.0 and SAINT+ version 6.01 area detector instrument control, data acquisition, and detector data integration software*; Bruker AXS, Inc.: Madison, WI, 2000.

(17) Sheldrick, G. M. *SHELXTL (SADABS, XS, XL) Crystallographic software Package, Version 6.10*; Bruker, AXS, Inc., Madison, WI, 2000.

Table 1. Crystal Data and Structure Refinement for Compounds **1** and **2**

molecular formula	$Mn[C_3NH_7(PO_3H_{0.5})]_4$	$Ni[C_3NH_6(PO_3H)]_4$-$[Ni(H_2O)_6]$
fw	601.24	769.78
cryst color, habit	colorless, needle	green, block
dimensions, mm^3	$0.32 \times 0.14 \times 0.03$	$0.17 \times 0.12 \times 0.11$
cryst syst	tetragonal	monoclinic
a, Å	12.349(2)	21.5524(14)
b, Å	12.349(2)	6.7015(5)
c, Å	14.066(4)	18.6491(12)
α, deg	90	90
β, deg	90	90.3660(10)
γ, deg	90	90
V, $Å^3$	2144.9(8)	2693.5(3)
space group	*P*4/*ncc*	*C*2/*c*
Z	4	4
ρ(calcd), c/g cm^{-3}	1.868	1.898
F(000)	1252	1600
θ range, deg	3.30−23.26	2.18−28.31
coeff, *μ*, mm^{-1}	0.986	1.724
T, K	110(2)	110(2)
λ, Å	0.71073	0.71073
no. reflns measured	8412 ($R_{int} = 0.0211$)	8135 ($R_{int} = 0.018$)
data/restrains/params	776/0/82	3109/0/185
refinement method	full-matrix least squares on F^2	full-matrix least squares on F^2
final *R* indices ($I > 2.0\sigma(I)$)	R1 = 0.0433 wR2 = 0.1257	R1 = 0.0371 wR2 = 0.0934
R indices (all data)	R1 = 0.0437 wR2 = 0.1262	R1 = 0.0397 wR2 = 0.0957
GOF on F^2	1.143 2.243; −0.460	1.115 1.313; −0.576

less than 1%. The structures were solved using direct methods (SHELXTL) and refined with full-matrix least-squares with atomic coordinates and anisotropic thermal parameters for all non-hydrogen atoms giving a final R1 value of 0.0443 for 82 parameters and 776 unique reflections with ($I > 2\sigma(I)$) and wR2 of 0.1267 for all 8412 reflections for **1** and a final R1 value of 0.0371 for 185 parameters and 3109 unique reflections with ($I > 2\sigma(I)$) and wR2 of 0.0957 for all 8135 reflections for **2**. An absorption correction was performed with SADABS. All hydrogen atoms were generated geometrically, assigned fixed isotropic thermal parameters, and included in the structure factor calculation. Refinement of complex **2** was satisfactory, and all atoms were ordered. However, there was a residual peak of 2.24 e $Å^{-3}$ (2.68 Å from O1) for complex **1** in the final difference Fourier map, which was located in the suitable hydrogen bonding distance within this peak and O1. When this peak was assigned as a disordered water molecule, it can be stabilized with the refinement of occupancy (50%). However, no water molecule was observed from TGA analysis clearly. We believe it was trace water which was trapped during the low-temperature data collection process. Also, this residue is located in the special position ($^1/_4$, $^1/_4$, 0.06). Some of the data collection and refinement parameters are summarized in Table 1. Important bond distances and angles for the two complexes are listed in Table 2.

Results and Discussion

Crystal Structure of $Mn[C_3NH_7(PO_3H_{0.5})]_4$, 1. 1,4,7,-10-Tetrakis(methylenephosphonic acid)-1,4,7,10-tetraazacyclododecane, DOTP, was reacted with $MnCl_2 \cdot 2H_2O$ hydrothermally at 150 °C in 1:1 molar ratio and yielded needlelike crystalline products which are clearly depicted in an SEM (scanning electron microscopy) reported as Figure 1. The single crystal diffraction result shows the manganese atom is tetrahedrally coordinated with four oxygen atoms from

Table 2. Selected Bond Lengths (Å) and Angles (deg) for Compounds **1** and **2**

Complex **1** Bond Lengths

Mn(1)−O(3)	2.020(3) 4×	P(1)−O(2)	1.517(3)
P(1)−O(3)	1.496(3)	P(1)−C(3)	1.820(4)
P(1)−O(1)	1.538(3)		

Complex **1** Bond Angles[a]

O(3)#1−Mn(1)−O(3)#2	122.12(15)	O(3)−Mn(1)−O(3)#3	122.12(15)
O(3)#1−Mn(1)−O(3)	97.82(18)	O(3)#1−Mn(1)−O(3)#3	109.40(18)
O(3)#2−Mn(1)−O(3)	109.40(18)	O(3)#2−Mn(1)−O(3)#3	97.82(18)

Complex **2** Bond Lengths

Ni(1)−O(1)	2.0684(2) 2x	Ni(2)−O(7)	2.0580(2) 2x
Ni(1)−N(1) 2×	2.1844(2)	Ni(2)−O(8) 2×	2.0611(2)
Ni(1)−N(2) 2×	2.1527(2)	Ni(2)−O(9) 2×	2.0517(2)
P(1)−O(1)	1.5060(2)	P(1)−O(2)	1.5063(2)
P(1)−O(3)	1.5784(2)	P(1)−C(1)	1.815(2)

Complex **2** Bond Angles[b]

O(1)#1−Ni(1)−O(1)	85.59(9)	O(9)#2−Ni(2)−O(9)	180.10(1)
O(1)#1−Ni(1)−N(2)	101.28(7)	O(9)#2−Ni(2)−O(7)	88.40(7)
O(1)−Ni(1)−N(2)	96.17(7)	O(9)−Ni(2)−O(7)	91.60(7)
N(1)−Ni(1)−N(1)#1	107.60(1)	O(7)#2−Ni(2)−O(7)	180.00(9)
N(2)−Ni(1)−N(2)#1	156.16(1)	O(9)#2−Ni(2)−O(8)#2	90.72(7)
O(1)#1−Ni(1)−N(1)	168.53(7)	O(7)−Ni(2)−O(8)#2	96.38(7)
O(1)−Ni(1)−N(1)	83.50(7)	O(7)#2−Ni(2)−O(8)#2	83.62(7)
N(2)−Ni(1)−N(1)	83.43(7)	O(8)#2−Ni(2)−O(8)	180.00(1)
N(2)#1−Ni(1)−N(1)	82.56(7)	N(2)#1−Ni(1)−N(1)#1	83.43(7)

[a] Symmetry transformations used to generate equivalent atoms: #1, $-^1/_2 - x, ^1/_2 - y, z$; #2, $y - ^1/_2, x + ^1/_2, ^1/_2 - z$; #3, $-y, -x, ^1/_2 - z$. [b] Symmetry transformations used to generate equivalent atoms: #1, $1 - x, y, ^1/_2 - z$; #2, $^1/_2 - x, ^3/_2 - y, -z$.

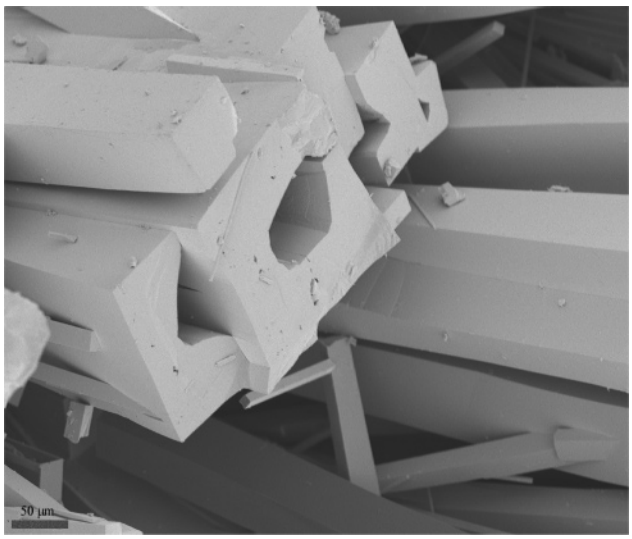

Figure 1. SEM image of compound **1**.

four different 1,4,7,10-tetrakis(methylenephosphonic acid)-1,4,7,10-tetraazacyclododecane ligands which are connected together to form a manganese infinite network along the *ab* plane as shown in Figure 2a. The bond distance between Mn and oxygen atoms is 2.020(3) Å. A Mn atom is located in the special position of $^3/_4$, $^1/_4$, $^1/_4$ which is shared by four different equivalent DOTP ligands. There are 22-membered rings positioned along the *c*-axis which are composed of 2Mn, 4N, 4P, 4O, and 8C atoms to form a porous material. The channels can be observed in the cell packing diagram in Figure 2b. The complexes are perfectly ordered with a 4-fold axis of symmetry. The P−O bond lengths 1.496(3), 1.517(3), and 1.538(3) Å, respectively, are all short. The

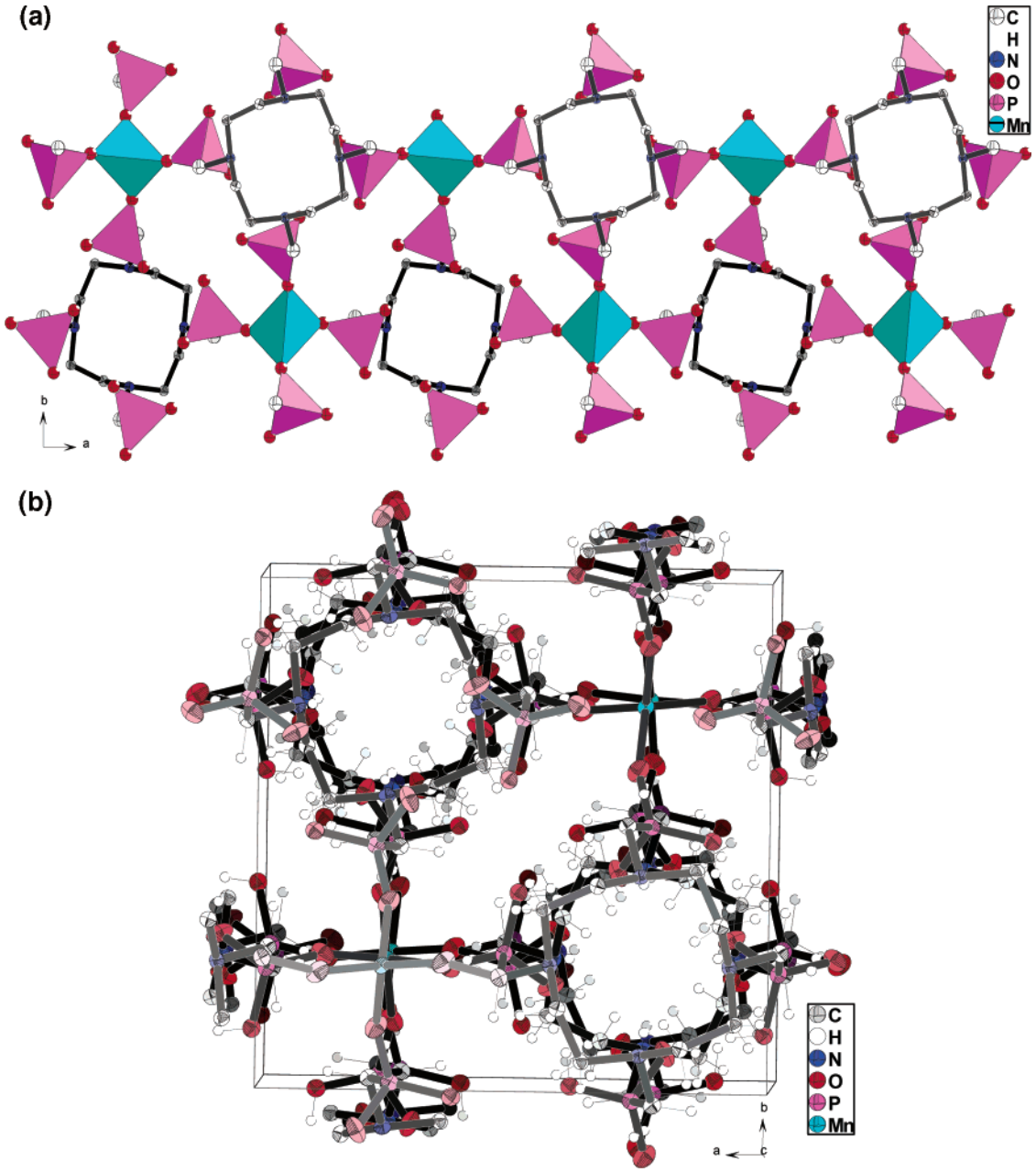

Figure 2. (a) Polyhedral diagram of compound **1** viewed down the *c*-axis (purple tetrahedron CPO_3 and cyan tetrahedron MnO_4). (b) Unit cell packing diagram of compound **1** in the *ab*-plane viewed down the *c*-axis.

shortest bond distance, P(1)−O(3), is involved in the coordination of the manganese atom, which is assumed to be an unprotonated P═O double bond or with a delocalized minus charge P- - -O bond. It seems that the proton H(1C) which is located on O(1) is disordered between O(1) and O(2)#4 (symmetry code: $y, {}^1/_2 - x, z$), because a very strong hydrogen bond 2.498(4) Å is formed between those two oxygen atoms with an ideal angle (160.5°). Also, for a hydrogen bonded to oxygen of a phosphonate group, the ideal P−OH bond is in the range 1.56−1.58 Å (see for example compound **2**). This bond length is slightly shorter in compound **1** at 1.538(3) Å again indicative of a disordered proton. The 12-membered macrocyclic cavity is empty with two protons pointed toward the cavity which forms a hydrophilic pocket. Scheme 1 also gives the schematic structure of compound **1**. The dotted lines circle the disordered hydrogen atoms. The 12-membered rings are connected by MnO_4 tetrahedra in an up and down notchlike fashion forming crenulated chains along the *ac*-plane as shown in Figure 3. The distance between two crown rings is 12 Å. On the basis of the bond valence calculation

$$\text{bv} = \exp(1.76 - 2.02)/0.37 = 0.495$$

(bv represents bond valence) (1)

$\sum$bv = 1.98, which indicated that the central manganese atom should be doubly charged.[18] The magnetic measurement confirmed that the compound is paramagnetic which is characteristic for compound **1**. The Mn(II) ions are isolated paramagnets. The data were fit to the Curie law, with C = 4.65 emu·K·mol^{-1}, in good agreement with the expected

(18) Brown, I. D.; Altermatt, D. *Acta Crystallogr.* **1985**, *B41*, 244.

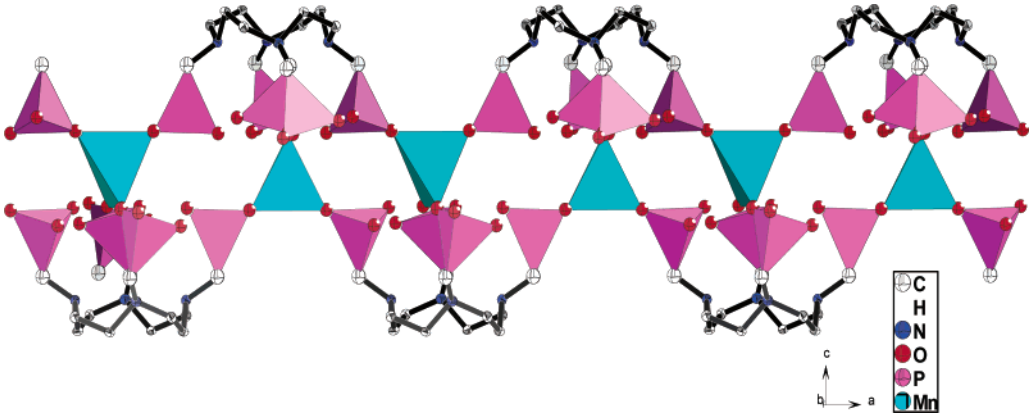

Figure 3. Polyhedral diagram of a single crystal of compound **1** viewed down the *b*-axis (purple tetrahedron CPO_3 and cyan tetrahedron MnO_4).

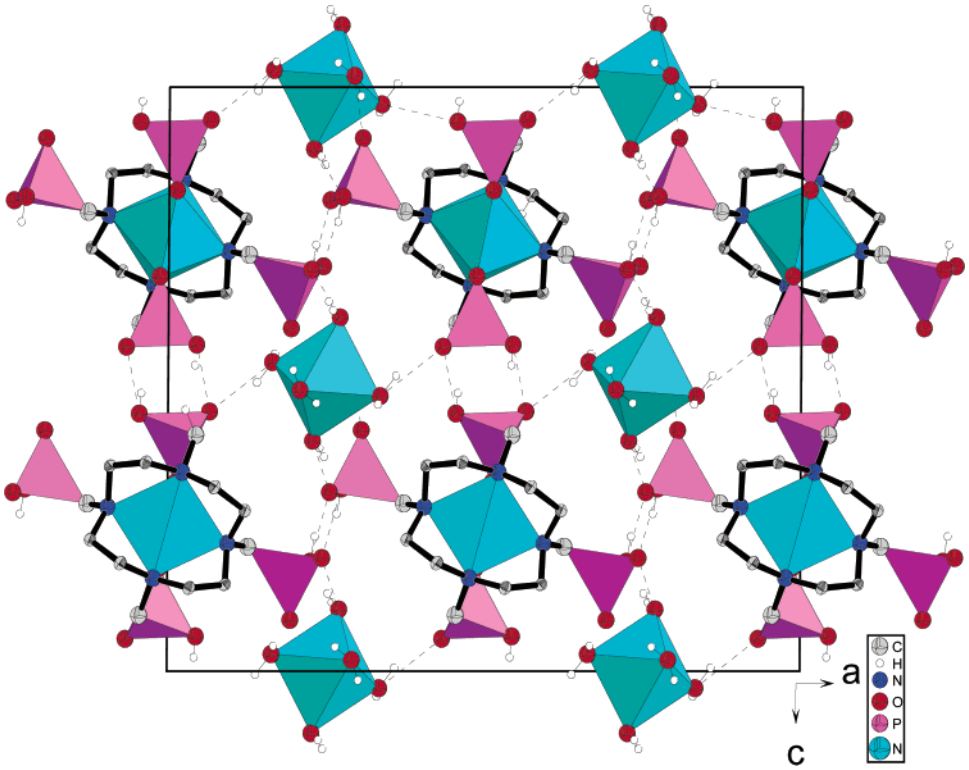

Figure 4. Polyhedral representation of the crystal structure of compound **2** along the *b*-axis (purple tetrahedron CPO_3 and cyan octahedron NiN_4O_2 and $Ni(H_2O)_6$).

value for isolated high spin Mn(II) ions ($S = {}^5/_2$ and $g = 2.06$) in a magnetically dilute sample. From the above information, the double positive charge was assigned to the central Mn. (See Supporting Information.)

Crystal Structure of $Ni[C_3NH_6(PO_3H)]_4[Ni(H_2O)_6]$, 2. The chemical formula of compound **2** in the crystal form, as obtained from the X-ray diffraction crystal structural analysis, is $Ni[C_3NH_6(PO_3H)]_4[Ni(H_2O)_6]$. The overall structure of the crystal is shown in Figure 4, where the asymmetric unit contains two different nickel centered moieties. Figure 5 shows the SEM image of the single crystal morphology for compound **2**. Compound **2** crystallized as an ion pair. The anion part is composed of $[Ni(1)(H_4DOTP)]^{2-}$ with octahedrally coordinated nickel. The ligand was deprotonated at the synthetic pH conditions (pH 6). Two methylene phosphonic acid pendent groups bend over and coordinate with the center nickel atoms in *cis* conformation. The N(1), N(1A), O(1), and O(1A) atoms are coplanar with a deviation 0.0585 Å, and the nickel atoms fit perfectly inside the equatorial plane. Two apical positions are filled with the other nitrogen atoms, N(2) and N(2A) of the aza-ring. A similar coordination environment was found for *cis-O,O*-$[Ni(H_2L)]$-$Cl{\cdot}H_2O$, *cis-O,O*-$[Ni(H_2L)]{\cdot}2H_2O$ (L = 1,4,8,11-tetraazacyclotetradecane-1,8-bis(methylphosphonic acid)).[19] Bond distances of P(1)−O(3) and P(2)−O(6) are 1.578(2) and 1.5705(2) Å, respectively, and are significantly longer than the coordinated P(1)−O(1) bonds and uncoordinated P(1)−O(2) (1.506(2) Å), P(2)−O(5) (1.5057(2) Å), P(2)−O(4) (1.5112(2) Å) bonds. Therefore, they have been designated as P−OH groups. As a result, each of the four phosphonate groups bonded to the aza-ring nitrogen has a single negative charge accounting for the anion double negative charge. The

(19) Kotek, J.; Vojtisek, P.; Cisarova, I.; Hermann, P.; Lukes, I. *Collect. Czech. Chem. Commun.* **2001**, *66*, 363

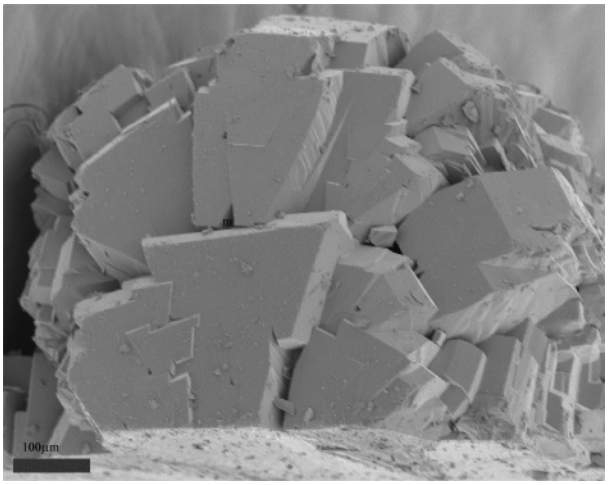

Figure 5. SEM image of compound **2**.

Ni cation octahedron $[Ni(H_2O)_6]^{2+}$ is composed of six coordinated water molecules with bond distances 2.052(2)−2.061(2) Å. All water molecules act as hydrogen donors and are hydrogen bonded with the phosphonate oxygen atoms. The hydrogen bonding network as shown in Figure 4 is viewed down the *b*-axis direction which runs through the *ac*-plane and forms infinite chains. Each phosphonate group connects to one proton, and two phosphonate moieties of neighboring complex molecules form a pair of intermolecular hydrogen bonds. The hydrogen bonds between the uncoordinated phosphonate oxygen groups O(6)−H···O(4)# 2.457(2) Å and the coordinated phosphonate oxygen groups O(3)−H···O(2)# 2.607(2) Å which result in an eight-membered ring $(P-O-H\cdots O-P)_2$ are shorter than those formed by water molecules (2.656(2)−2.751(2) Å). The complex molecules, connected through the hydrogen bonds, form infinite chains very similar to those found in the structure of *cis-O,O*-$[Ni(H_2L)]Cl\cdot H_2O$, *cis-O,O*-$[Ni(H_2L)]\cdot 2H_2O$, *trans-O,O*-$[Co(HL)]\cdot 3H_2O$, *trans-O,O*-$[Co(HL)]\cdot 3H_2O$ (L = 1,4,8,11-tetraazacyclotetradecane-1,8-bis(methylphosphonic acid)),[20] and $Cu(H_2L^1)$ (L^1 = *N,N′*-bisphosphonomethyl-1,10-diaza-18-crown-6).[2c]

Ion Exchange. Compound **1** was tested for ion exchange for the Cs^+. The hydrophilic pocket with exchangeable protons on the ring and P−OH groups as shown in the structure may accommodate large ions such as Cs. A total of 50 mg of the sample (crystals) was shaken with 8.55 mmol/L CsCl solution for 48 h. The initial pH of the solution was 5.22 and changes to 3.76. The result of AA analysis showed that compound **1** picked up 0.182 mmol/g Cs^+ from the solution. Protons were released to the solution after ion exchange as evidenced by the pH measurements. About 11% of the protons were exchanged by Cs^+ ions. Single crystal data on the exchanged crystal were collected after ion exchange. The result showed that the cell had the same unit cell parameters: $a = 12.3390(11)$ Å, $b = 12.3390(11)$ Å, $c = 14.0406(2)$ Å, $V = 2137.7(5)$ Å^3, $Z = 4$. No peaks associated with Cs^+ scattering were observed. The structure was resolved, and no Cs was found in the resolved structure.

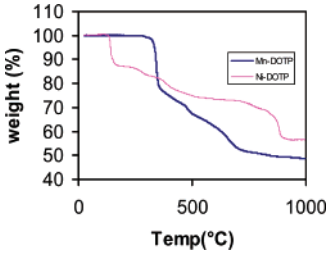

Figure 6. TGA curves for compounds **1** and **2**.

The adsorption of cesium occurred most likely only on the surface of the crystalline material. It is difficult to tell whether the Cs exchanged with the protons on the 12-membered ring or with the P−OH groups attached to the ring. In this experiment, crystals were used for ion exchange which may reduce the capability of the material to exchange of Cs^+ because of difficulty in diffusion into the lattice. More confirmative experiments will be reported in the future.

Thermogravimetric Study. The thermogravimetric studies of compound **1** demonstrated a number of weight losses indicating a complexity of the decomposition process (Figure 6). According to the structural data, no water molecules were found in the compound. The TGA diagram shows that there is no weight loss till 358 °C confirming that the residual peak in the final Fourier map can be assigned to surface water in the X-ray analysis data collection. The burning of the organic part and phosphonic acid hydroxyl group condensation start at 358 °C and continue until 1000 °C.[21] The total weight loss of 51.4% corresponds to the final residue being $Mn_2P_2O_7$ (52.6%). The TGA curve of compound **2** has two weight loss regions. Compound **2** starts losing the coordinated water at 170 °C indicating a high temperature of dehydration because of the strong bonding of water molecules to the metal atom. The observed weight loss at 275 °C (14.1%) is in agreement with the calculated value of 14.0% for all six coordinated water molecules. There are two small regions of weight loss (9.7%) in the temperature range 275−450 °C which could be assigned to a condensation of the hydroxyl groups in DOTP ligand with a theoretical weight loss value of 9.35%. The burning of the organic ligand and transformation of phosphonic moieties occur at 450−900 °C. The process is complete with a total weight loss value of 43.4%, in a good agreement with the calculated final residue $Ni_3(PO_4)_2$ + NiO (42.7%).[22−24]

IR Study. IR spectra were recorded between 4000 and 400 cm^{-1} and are shown in Figure 7. The region between 4000 and 1400 cm^{-1} can be selected to study the coordinated water and the P−O−H groups. Two bands observed at 2760 and 2340 cm^{-1} which are likely due to the ν(PO−H) and 2δ(POH), respectively, are characteristic of hydrogen phosphonate groups and more intense for compound **2** in agreement with its stoichiometry. Compound **2** showed an intense and broad band in the O−H stretching vibration

(20) Kotek, J.; Lubal, P.; Hermann, P.; Cisarova, I.; Lukes, I.; Godula, T.; Sovbodova, I.; Taborsky, P.; Havel, J. *Chem. Eur. J.* **2003**, *9*, 233.
(21) Zhang, B.; Poojary, D. M.; Clearfield, A. *Inorg. Chem.* **1998**, *37*, 1844.
(22) Poojary, D. M.; Zhang, B.; Bellinghausen, P.; Clearfield, A. *Inorg. Chem.* **1996**, *35*, 4942.
(23) Poojary, D. M.; Zhang, B.; Bellinghausen, P.; Clearfield, A. *Inorg. Chem.* **1996**, *35*, 5254.
(24) Menaa, B.; Shannon, I. J. *J. Mater. Chem.* **2002**, *12*, 350.

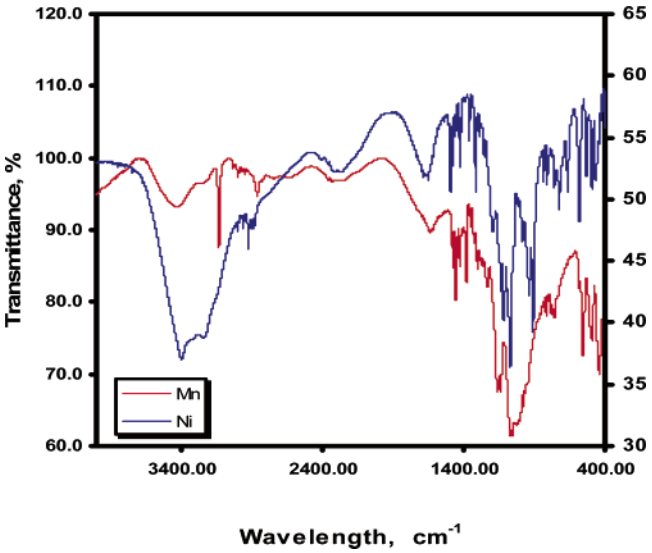

Figure 7. IR spectra of compounds **1** and **2**.

region at 3410−3250 cm^{-1}, which is consistent with the presence of coordinated water interacting by H-bonding. The corresponding bending H−O−H (δHOH) vibration of the coordinated water is located at ca. 1684 cm^{-1}, which is also broadened by hydrogen bonding. In fact, the band at 1680 cm^{-1} is close to the maximum 1690 cm^{-1} which is usually assigned to the bending vibrations of species containing highly mobile protons, and is typical of good protonic conductors.[25] A sharp band was observed at 3135 cm^{-1} for compound **1** which is due to the stretching vibration of the N−H group in the macrocyclic ligand and a bending vibration band at 1635 cm^{-1} indicating the existence of protonated NH^+ and is in agreement with the X-ray structural analysis. As we have pointed out, compound **1** is anhydrous, so the band of 1635 cm^{-1} is not due to hydration water. Also, two kinds of ν_{as} of PO_3 were observed in compound **1** at 1097 and 1054 cm^{-1}, respectively. The peak that occurs at 982 cm^{-1} was assigned to $\nu_s(PO_3)$.[26] The bands centered at 2330 and 1075 cm^{-1} are attributed to (PO−H) and (POH) vibrations, respectively, due to unprotonated POH groups in both compounds. Asymmetric vibrating stretching bands of POH (ν(P−OH)) groups are situated at 980 cm^{-1}. Both compounds showed typical C−H stretching vibrations and bending vibrations of low intensities of CH_2 both inside the ring and/or attached to nitrogen atoms, near 2850 and 1478 cm^{-1}, respectively. The νP−C vibration bands of compound **1** are located at 1382 cm^{-1}; otherwise, the similar bands for compound **2** are split into two bands and are separately situated at 1360 and 1316 cm^{-1}, respectively, due to two different kinds of phosphonic pendent groups involved. One is coordinated with the nickel atom and the other is not.

Conclusions

Two new different types of metal phosphonates have been synthesized and characterized by X-ray diffraction, magnetic measurements, IR spectroscopy, and TGA measurements. Both structures have been solved from X-ray single crystal data. It has been demonstrated that the tetrahedrally coordinated Mn centers are shared by four oxygen atoms from neighboring pendent phosphonic acid groups which are associated with the 12-membered aza-ring. The nitrogen atoms are not involved in the coordination at compound **1**. It forms a 2D array along the *c*-axis. The hydrophilic cavity of the aza-crown is empty and accessible by other cations. Preliminary ion exchange studies showed that compound **1** picked up Cs^+ from the solution. Its powder form will further be screened for exchange of other cations. Compound **2** contains two different octahedrally coordinated Ni centers with hydrogen bonding extended to form 2D infinite chains in the *ac*-plane, in which a six-water-coordinated nickel ion is clathrated and acts as counterion to the negatively charged $[Ni(H_4DOTP)]^{2-}$ motif. Both compounds show the typical paramagnetic properties. In the case of the manganese compound, the pH was kept acidic (pH $\sim$ 2); as a result, four protons of the initial eight on the phosphonate groups are donated to the four aza nitrogens and two are displaced by the Mn^{2+} ions. The two remaining protons are shared equally by the four phosphonate groups in accordance with the symmetry requirements. Because the aza groups are protonated, the Mn^{2+} reacted with the phosphonate groups rather than with the aza crown ring. In the case of the nickel compound, the protons were essentially removed from the aza nitrogens leaving just one proton on each of the four phosphonic acid groups. Thus, two Ni^{2+} ions were required to neutralize the ligand, one being coordinated by the ring and phosphonate groups and the other forming a hexahydrate. The compound is essentially ionic with an extensive system of hydrogen bonding. These reactions should be general for aminophosphonate ligands. We have prepared a series of aza crown ethers with appended phosphonic acid groups in a variety of ring sizes.[27] By careful control of the proton removal, families of new compounds with metals or amine linkers should be achieved. Furthermore, compounds that retain protons may be manipulated to exchange and coordinate or selectively separate ions or neutral species.

Acknowledgment. The authors acknowledge with thanks the financial support from the Department of Energy, Basic Sciences Division, through Grant DE-FG03-00ER 15806. Thanks to Dr. Naima Bestaoui for assistance in obtaining SEM pictures and Drs. Yang Li and Andrey Prosvirin for magnetic measurements.

Supporting Information Available: Crystallographic data, including CIF files, and magnetic measurements. This material is available free of charge via the Internet at http://pubs.acs.org.

IC040076M

(25) Martinez-Tapia, H. S.; Cabeza, A.; Bruque, S.; Pertierra, P.; Garcia-Granda, S.; Aranda, M. A. G. *J. Solid State Chem.* **2000**, *151*, 122.
(26) (a) Barja, B. C.; Herszage, J.; Santos Alfons, M. *Polyhedron* **2001**, *20*, 1821. (b) Cabeza, A.; Aranda, M. A. G.; Bruque, S. *J. Mater. Chem.* **1999**, *9*, 571. (c) Gomez-Alcantara, M. M.; Cabeza, A.; Aranda, M. A. G.; Guagliardi, A.; Mao, J. G.; Clearfield, A. *Solid State Sci.* **2004**, *6*, 479.
(27) Kong, D. Y.; McBee, J.; Clearfield, A. Unpublished work.